Journal of Engineering and Applied Sciences 13 (22): 9540-9547, 2018
ISSN: 1816-949X

# Special Properties for Resistance to Corrosion of Biomedical Alloy Ti-Al-Mo-Zr Used in Surgical Operations

Jassim Mohammed Salman Al-Murshdy
College of Materials Engineering, Babylon University, Hillah, Iraq

**Abstract:** Ti-1.25% Al-0.75% Mo-1% Zr base alloy was prepared with a lower weight percentage then the standard alloy. The other 3 alloys were worked after adding the Chromium (Cr) and Nickel (Ni) elements separately and collecting them together to the base alloy using powder metallurgy technique. The corrosion tests of the alloys were carried out with Saliva and Hanks solutions, also, the hardness tests, X-ray, microstructure through using Scaning Electron Microscopy (SEM) Light Optical Microscopy (LOM) and Atomic Force Microscopy (AFM). The outcomes was showed that the addition of the chromium element improved resistance to corrosion for both solutions by 28% Saliva and 40% Hanks for base alloy. Also, the combination of the 2 elements gives higher improvement corrosion resistance via., compared with the base alloy and addition nickel alone. Morever, the results of microstructure was indicated that the increased of β phase of Ti-1.25% Al-0.75% Mo-1% Zr-0.5% Cr alloys while the hardness results were showed increasing with addition elements, X-ray indicated that new phases. As well the nature of corroded surfaces had a little different from the uncorroded during the tests of the atomic force microscopy for most used alloys studied.

**Key words:** Biomedical alloys, corrosion resistance, Ti-alloys, powder metallurgy, hardness, microcopy

## INTRODUCTION

The field of biomedical materials was become very important because these materials can improve the life and increase in human age (Elshalakany *et al*., 2017). The main reason for the use of titanium alloys in medical applications is the high strength with a suitable ductility in relation to its light weight compared with Cobalt-Crome and stainless steels alloys, titanium alloys are therefore, expected to be widely used in bone implants (Ahmed *et al*., 2014; Hussein *et al*., 2015). A unique feature of titanium with other alloys such as Cobalt Chrome alloys it is more suitable for medical applications because of its high resistance and compatibility and resistance to corrosion which especially enjoy it (Licausi *et al*., 2013). The high compatibility of these alloys is the main reason for their use more visually than in other medical or dental fields (Li *et al*., 2014). The behavior of excellent titanium alloys made it one of the important choices in the medical side because of the characteristics of mechanical and behavior of corrosion due to the layer of oxide compatible with the human body in addition to light weight and low coefficient of youngs and behavior of non-magnetism (Peng *et al*., 2016).

Titanium-based alloys are widely used as biomedical materials on the other hand, metallic materials can not be substituted for polymers and ceramics nowadays because high resistance and corrosion resistance are among the most outstanding requirements for the safety of biomedical materials (Hanawa, 2006). The use of titanium alloys due to its excellent mechanical properties, so, attempts to develop them to include greater compatibility between them and the blood and the nature of the surrounding tissue in addition to adding new elements.

The new developments must be based on metal and preferably there is a good balance between corrosion resistance and the mechanical properties of the alloy produced (Lastnosti *et al*., 2017; Hsu *et al*., 2015). When compared with other alloys, titanium alloys were considered to be the best materials for their superior properties in medical applications and in bone implants on other competing materials (Lin *et al*., 2017). Ti alloys were classified into three simple types which contain (α, β and α+β) some elements were dissolved preferentially in (α) phase such as Zr, Al, Sn, O and Si raising in (α+β) phase. The addition of these elements results in the modulation of the alloy properties such as hardening and corrosion resistance improvement, these are suitable for biomedical application, this is due to of their high specific strength and low modulus (Mohan *et al*., 2012).

Some elements stabilize the (β) phase and depress (α+β) phase. These fall into two groups (β) eutectoid and (β) isomorphous. Hydrogen, molybdenum, tungsten and vanadium stabilize the (β) phase while oxygen, nitrogen and carbon promote the (α) phase (Jackson and Dring (2006).

Powder metallurgy technology has the advantages of design in shape a way that contributes to making the granules softer and thus, homogeneous microstructure (Ho *et al*., 2012). Adding different alloying elements like (Zr, Cr) this has a great effect on properties to improve the strength (Oliveira and Guastaldi, 2009). Additions of chromium and nikel also will be expand phase (β) at the expense of other phases. In this study, these elements were selected as additional elements, this is because its improve the properties especially resistance to corrosion and its tendency toward stability and passivate.

## MATERIALS AND METHODS

### Experimental work

**Alloys preperation for compacting and sintering:** The purity of metals powders were used to prepare the biomedical alloys in this study as the following, 99.93%Ti, 99.95% Cr, 99.77Mo, 99.88 Al, 99.78% Ni and 99.82% Zr. Powder metallurgy technique was used to prepare the alloys. The procedure involves mixing, compacting and sintering. Table 1 shows the chemical composition and code of the alloys which were used in this study.

Sensitive balance with (±0.0001 accuracy) was used to weight for each amount of the powders before mixing. The mixing process was being carried out for 2 h. The die was used in the alloys preparation process the cylindrical one direction action die with diameters (12.8) mm 0.650 MPa was the stress applied on the metallic powders in order to get green compacting alloys by using the electric hydraulic press.

The sintering process was carried out under the vacuum conditions through using the vacuum tube furnace.the sintering system consists of a tube furnace and rotary vacuum up to $10^{-4}$ torr. The alloys of sintering process including the following:

- Heating from room temperature to 550°C
- Soaking for 3 h at 550°C
- Heating from temperature 550-850°C
- Soaking for 5 h at 850°C
- Slow cooling in the furnace with continues vacuum to the room temperatures

Table 1: The chemical composition and code of the prepared alloys

| Code of alloy | Chemical composition (wt.%) |
|---|---|
| A | Ti-1.25% Al-0.75% Mo-1% Zr (base alloy) |
| B | Base alloy+0.5% Cr |
| C | Base alloy+0.25% Ni |
| D | Base alloy+0.5% Cr+0.25% Ni |

Table 2: Chemical composition of etching solution (Nadai *et al*., 2013)

| Constituent | Values (mL) |
|---|---|
| HF | 10 |
| $HNO_3$ | 5 |
| Water | 85 |

Table 3: Chemical composition of Saliva solution (Tamilselvi and Rajendran, 2006)

| Constituent | Values (g/L) |
|---|---|
| KCl | 1.5 |
| Na $HCO_3$ | 1.5 |
| $NaH_2PO_4H_2O$ | 0.5 |
| HSCN | 0.5 |
| Lactic acid | 0.9 |

Table 4: Chemical composition of Hank's solution (Tamilselvi and Rajendran, 2006)

| Constituent | Values (g/L) |
|---|---|
| KCl | 0.40 |
| $CaCl_2$ | 0.14 |
| NaCl | 8.00 |
| $NaHCO_3$ | 0.35 |
| Glucose | 1.00 |
| $MgCl_2.6H_2O$ | 0.10 |
| $Na_2HPO_4.2H_2O$ | 0.06 |
| $KH_2PO_4$ | 0.06 |
| $MgSO_4.7H_2O$ | 0.06 |

**Alloys preparation for testing:** All alloys after sintering process were grinded via using grit silicon carbide papers, then polished with a diamond past to get a bright mirror finish for the final step. Etching was made at room temperature, Table 2 shown the chemical composition of the etching solution (Nadai *et al*., 2013). After etching process the alloys were washed with water and dried.

The microstructures were used alloys after the sintering process via using a light optical, atomic force microscopy using scanning prob microscopy AFM (AA3000) contact mode and scaning electron microscopy. The microstructure was evaluated with (100 and 400x) magnification via. using Olympus microscope. The scanning electron microscope examination were used to reverse the microstructure of alloys after sintering. The X-ray diffraction techniques were taken for the alloys upon using XRD instrument. X-ray diffraction test was conducted for the alloys after sintering process, scanning speed 2°/min was used. About 30°-80° the range of the diffraction angle, Brinell tester was used to measure of the hardness of the alloys with 40 kg/mm$^2$ as applying weight and the incubation time was 10 sec in state applied weight. Three readings for each alloy was taken and the average value was used to analysis of the behavior of the alloys.

The corrosive behavior of alloys studied in 2 different solutions (Saliva and Hank's solution). The composition of Saliva and Hank's solution was illustrated in Table 3 and 4, respectively (Tamilselvi and Rajendran, 2006). The pH of Saliva and Hank's solution at 37°C were 6.7 and 7.4, respectively.

## RESULTS AND DISCUSSION

**Partical size analyzer:** The average particle size of metal powders (Ti, Al , Mo, Zr , Cr and Ni) ranges from (20-40) μm as shown in Fig. 1 average partical size as the following: (28.82Ti, 40.03Cr, 21.40Mo, 28.45Al, 29.65Ni and 24.01 μm Zr) from Fig. 1, we can show that the sizes are small and this produces a homogeneous bonding of alloys in the compacting and also notes that red curve represent method of distribution powders and blue curve deales with accumulated distribution of powders.

**Effect of the sintering alloys on the microstructure and phases:** Figure 2 shows the microstructure of alloys (a-d) after sintering under scanning electron microscopy and Fig. 3 shows the microstructure of same alloys by an optical microscopy. In Fig. 2 and 3a-d found that, the all alloys contain (α) and (β) phases, the darker area (β) phase while the whiter area α phase. Moreover, it can also be seen in the microstructure, there are a few porosities which vary in size and shape. The grain boundaries become clearer when analyzing of the optical microscopy, add to that the fine microstructure of the titanium alloys increases the strength and hardness and delay the growth of the crack and corrosion and this needed in the biomedical alloys.

Figure 4 represnt X-ray diffraction pattern for A alloy after the sintering process before sintering no phases transformation takes place during compacting. The presence of some phases $AlTi_2$, $AlTi_3$ and others show how is the effective these phases are in improving the properties of alloys. The current study showed that the small amounts of the phases did not appear in Fig. 4 and this is because of small proportions and small sizes, this phenomenon applies to others alloys b-d.

**The potentiodynamic polarization for alloys:** The study of polarization behavior of alloys in different solutions (Saliva and Hanks) involves the active region which consists of cathodic and anodic region to calculate the corrosion potentials and corrosion current densities. The cathodic region represents the reduction reaction which occurs on surface of alloy while the anodic represent the dissolution of metal or metals in alloy to ions. One of the important ways to study the behavior of corrosion is the formation of the film and protective layer of alloys in the solutions. The potential increase in the positive direction, The steady state of the potential was indicated that this layer is intact and protective. The resistance of the protective layer of corrosion depends on addition elements for base alloy and formation oxide layer (Choubey *et al*., 2005). Figure 5 shown curves of Potentiodynamic polarization for alloys (Fig. 5a-d) at 37°C in Hanks solution.

The base alloy has a corrosion potential (-237 mV) and current (77.25 μA) while the B alloy has a corrosion potential (-122 mV) and current (46.47 μA) and because the presence of Cr element in this alloy it works to control the anodic reaction and tends to formation the passive layer from corrosion, the resistance to corrosion of alloy B is the highest in compared with alloys were used at approx. 40% from base alloy in Hanks solution as all these alloys work on formation Ti Oxide ($TiO_2$) on surface of alloys and thickness of the layer is dependent on formation oxide. As well as structure added Ni element improved corrosion resistance for C alloy which has corrosion potential (-295 mV) and current (60.24 μA) but with lower values from B alloy but the highest from the base by 22% either combine the two elements together Cr and Ni improved the alloy D by 33% from C and base alloy.

This study shown that the base alloy A has corrosion potential and the current different from base alloy for the Hanks solution. The presence of the strong passivating elements like Cr and Ni in alloys the cause of high corrosion resistance in these alloys, the $TiO_2$, $Al_2O_3$ and $ZrO_2$ are working on formation passive layer of alloys (Hsu *et al*., 2015) thus, this is improved corrosion resistance of B alloy by 28%, from Fig. 6c, d it was observed that some curves exhibited active-passive behavior with the formation of protective layers in the compared with the results of corrosion in both solutions. However, the results of the corrosion resistance in Hanks were higher than in Saliva solution.

Figure 7 shows that the surface microstructure of alloys after corrosion, Fig. 7a-d show that the surface corrosion at most alloys very little or perhaps is not corrosive this is because the nature of the surface that were protected by film layer, so, it appears the microstructure of corroded surface almost similar to un corroded surface of alloys this phenomenon is prevalent in Hanks solutions.

Figure 8 shows that the surface microstructure of Atomic Force Micrscopy (AFM) for the corroded area in A and B alloys, the roughness average 53.5 nm for A alloy and 36.6 nm for B alloy, image surface area 21091883.42 and 16875336.72 for A and B, respectively, from the results, we can shows that the suface does not affect or little affected and remainded as it is and this is due to the protective layers as mentioned.

**Effect of elements addition on hardness:** Figure 9 shows that the hardness versus elements addition, the hardness was increased significantly with addition of elements and differently according to each alloy and due to the surface hardness of these alloys in compared with base alloy

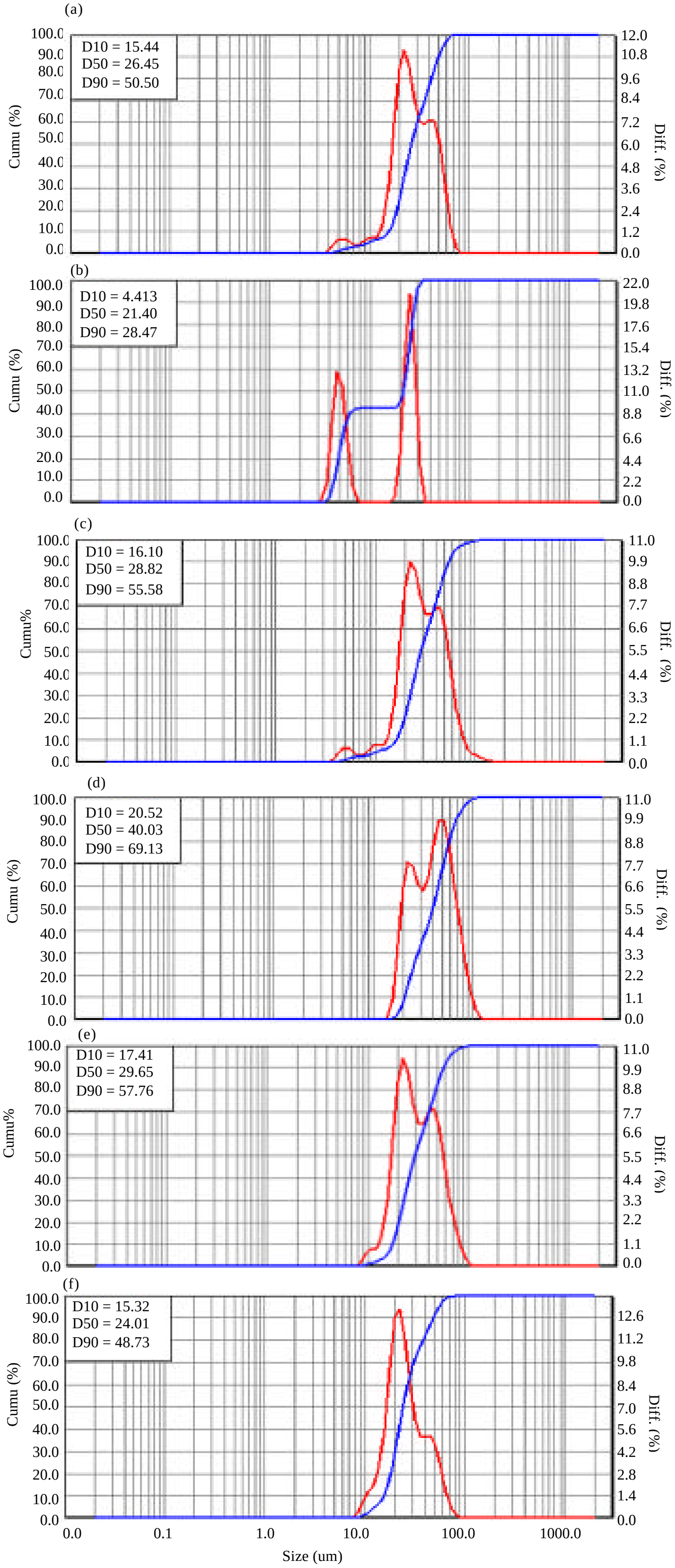

(a)

| Diam (µm) | Percent |
|---|---|
| 0.200 | 0.00 |
| 0.500 | 0.00 |
| 1.000 | 0.00 |
| 0.200 | 0.00 |
| 0.500 | 1.12 |
| 10.000 | 4.87 |
| 20.000 | 25.14 |
| 45.000 | 83.40 |
| 75.000 | 99.87 |
| 100.000 | 100.00 |

(b)

| Diam (µm) | Percent |
|---|---|
| 0.100 | 0.00 |
| 0.200 | 0.00 |
| 0.500 | 0.00 |
| 1.000 | 0.00 |
| 2.000 | 0.00 |
| 5.00 | 23.43 |
| 10.000 | 42.48 |
| 20.000 | 45.78 |
| 45.000 | 100.00 |
| 75.000 | 100.00 |

(c)

| Diam (µm) | Percent |
|---|---|
| 0.500 | 0.00 |
| 1.000 | 0.00 |
| 2.000 | 0.00 |
| 5.000 | 1.14 |
| 10.000 | 4.32 |
| 20.000 | 21.75 |
| 45.000 | 77.97 |
| 75.000 | 97.61 |
| 100.000 | 99.25 |
| 20.000 | 100.00 |

(d)

| Diam (µm) | Percent |
|---|---|
| 0.500 | 0.00 |
| 1.000 | 0.00 |
| 2.000 | 0.00 |
| 5.000 | 0.00 |
| 10.000 | 0.00 |
| 20.000 | 8.54 |
| 45.000 | 58.78 |
| 75.000 | 93.24 |
| 100.000 | 99.38 |
| 20.000 | 100.00 |

(e)

| Diam (µm) | Percent |
|---|---|
| 0.500 | 0.00 |
| 1.000 | 0.00 |
| 2.000 | 0.00 |
| 5.000 | 0.00 |
| 10.000 | 0.70 |
| 20.000 | 19.00 |
| 45.000 | 75.59 |
| 75.000 | 97.70 |
| 100.000 | 99.92 |
| 20.000 | 100.00 |

(f)

| Diam (µm) | Percent |
|---|---|
| 0.200 | 0.00 |
| 0.500 | 0.00 |
| 1.000 | 0.00 |
| 2.000 | 0.00 |
| 5.000 | 0.00 |
| 10.000 | 1.11 |
| 20.000 | 30.30 |
| 45.000 | 86.50 |
| 75.000 | 99.66 |
| 100.000 | 100.00 |

Fig. 1a-d: Partical size analyzer of powders Ti, Al, Mo, Zr, Cr and Ni, respectively

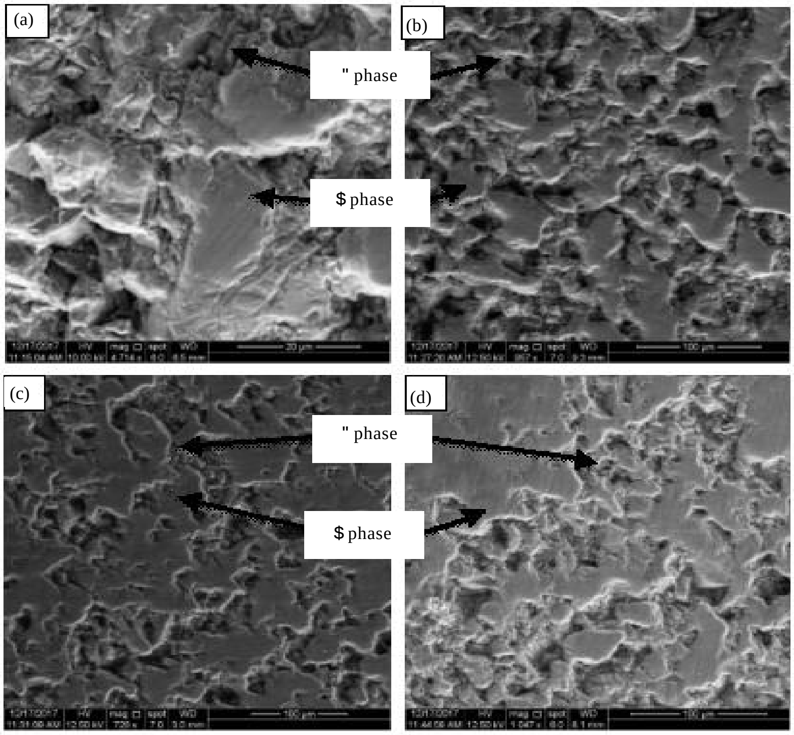

Fig. 2a-d: SEM for alloys after sintering

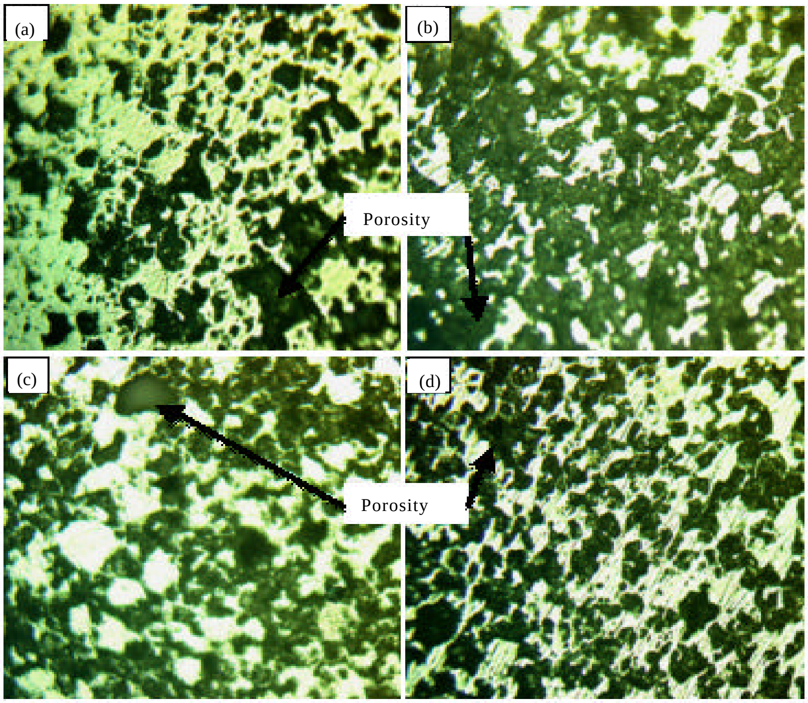

Fig. 3a-d: LOM for after sintering

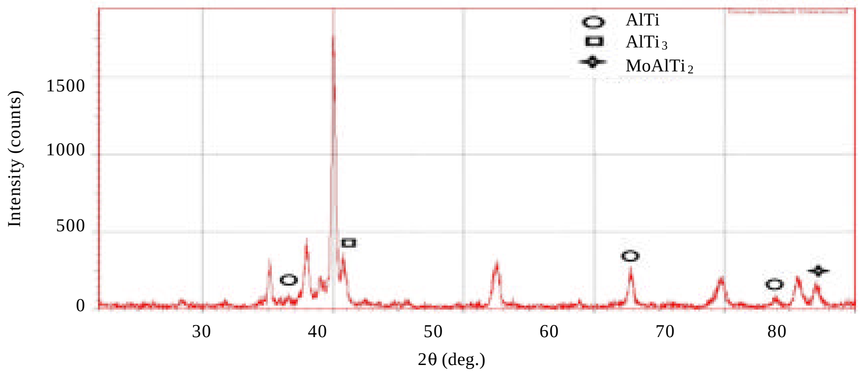

Fig. 4: XRD for A alloy after sintering process

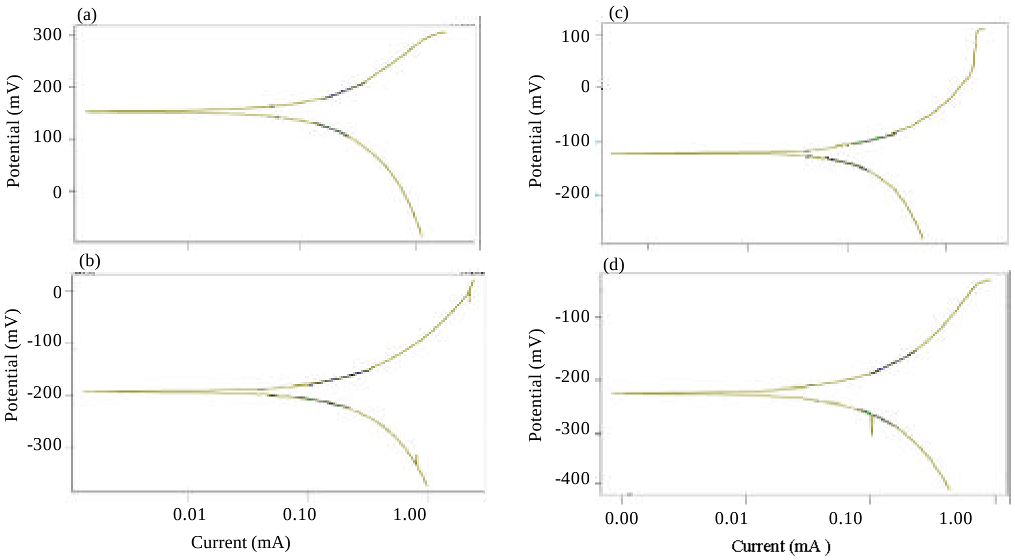

Fig. 5a-d: The curves of potentiodynamic polarization for the alloys in Hanks solution at 37°C

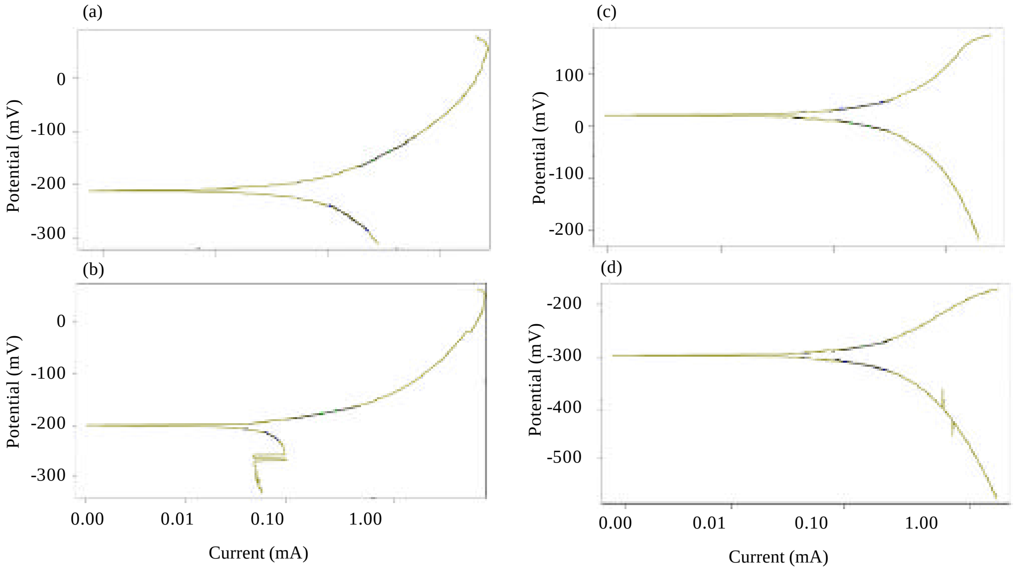

Fig. 6a-d: The curves of potentiodynamic polarization for alloys in Saliva solution at 37°C

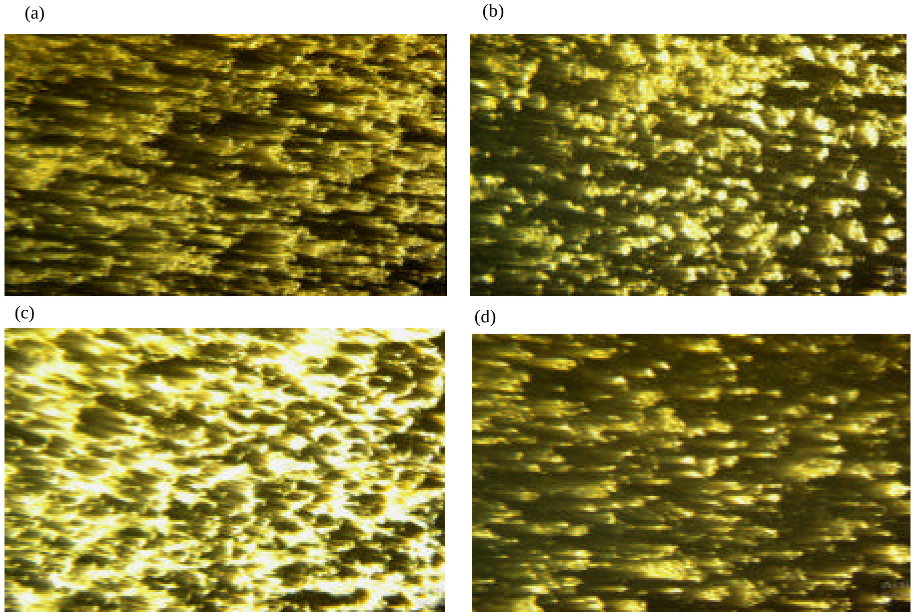

Fig. 7a-d: The surface microstructure of alloys after corrosion

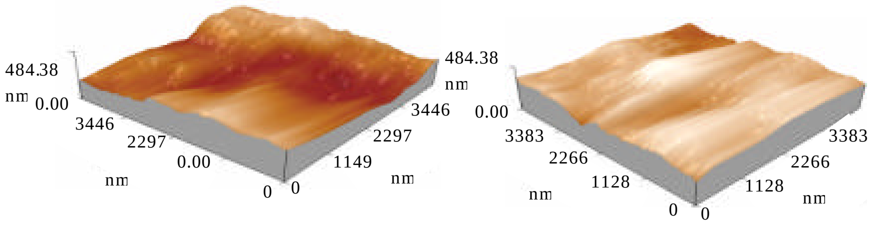

Fig. 8: Surface corrosion of atomic force microscopy for A and B alloys

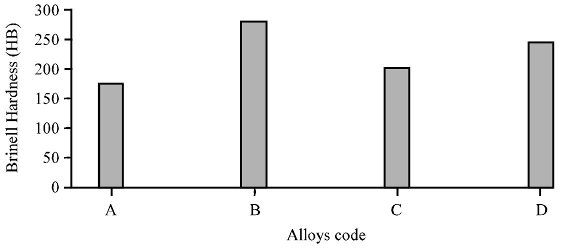

Fig. 9: The hardness versus elements addition

because the oxides. However, it was known that the Ti alloys improved hardness as improved corrosion resistance (Lastnosti *et al.*, 2017) these results are consistent with previous results obtainded.

## CONCLUSION

- Additions Cr and Ni showed that improving corrosion resistance of alloys
- The best corrosion resistance was achieved for Ti-Al-Mo-Zr-Cr alloy in both solutions (Hanks and Saliva)
- The hardness was increased significantly in compared with base alloy
- New phases observed in the microstructure and X-ray diffraction for alloys
- Both solutions (Hanks and Saliva) improved the properties of alloys but Hanks solution higher than saliva solution

## REFERENCES

Ahmed, M., D.G. Savvakin, O.M. Ivasishin and E.V. Pereloma, 2014. The effect of ageing on microstructure and mechanical properties of powder Ti-5Al-5Mo-5V-1Cr-1Fe alloy. Mater. Sci. Eng. A, 605: 89-97.

Choubey, A., B. Basu and R. Balasubramaniam, 2005. Electrochemical behavior of Ti-based alloys in simulated human body fluid environment. Trends Biomater. Artif. Organs, 18: 64-72.

Elshalakany, A.B., S. Ali, A.A. Mata, A.K. Eessaa and P. Mohan *et al*., 2017. Microstructure and mechanical properties of Ti-Mo-Zr-Cr biomedical alloys by powder metallurgy. J. Mater. Eng. Perform., 26: 1262-1271.

Hanawa, T., 2006. Recent development of new alloys for biomedical use. Mater. Sci. Forum, 512: 243-248.

Ho, W.F., S.C. Wu, S.K. Hsu, Y.C. Li and H.C. Hsu, 2012. Effects of molybdenum content on the structure and mechanical properties of as-cast Ti-10Zr-based alloys for biomedical applications. Mater. Sci. Eng. C, 32: 517-522.

Hsu, H.C., S.C. Wu, S.K. Hsu, C.T. Li and W.F. Ho, 2015. Effects of chromium addition on structure and mechanical properties of Ti-5Mo alloy. Mater. Des., 65: 700-706.

Hussein, M.A., A.S. Mohammed and N. Al-Aqeeli, 2015. Wear characteristics of metallic biomaterials: A review. Mater., 8: 2749-2768.

Jackson, M. and K. Dring, 2006. A review of advances in processing and metallurgy of titanium alloys. Mater. Sci. Technol., 22: 881-887.

Lastnosti, V.L.E.N.M., O.K. Zlitine and P.Z.M. Prahov, 2017. Influence of alloying elements on the mechanical properties of a cobalt-based alloy produced with powder metallurgy. Mater. Technol., 51: 443-447.

Li, Y., C. Yang, H. Zhao, S. Qu and X. Li *et al*., 2014. New developments of Ti-based alloys for biomedical applications. Mater., 7: 1709-1800.

Licausi, M.P., A.I. Munoz and V.A. Borras, 2013. Influence of the fabrication process and fluoride content on the tribocorrosion behaviour of Ti6Al4V biomedical alloy in artificial saliva. J. Mech. Behav. Biomed. Mater., 20: 137-148.

Lin, J., S. Ozan, K. Munir, K. Wang and X. Tong *et al*., 2017. Effects of solution treatment and aging on the microstructure, mechanical properties and corrosion resistance of a ß type Ti-Ta-Hf-Zr alloy. RSC. Adv., 7: 12309-12317.

Mohan, L., C. Anandan and V.W. Grips, 2012. Corrosion behavior of titanium alloy Beta-21S coated with diamond like carbon in Hank's solution. Appl. Surf. Sci., 258: 6331-6340.

Nadai, L., B. Katona, A. Terdik and E. Bognar, 2013. Chemical etching of titanium samples. Periodica Polytech. Eng. Mech. Eng., 57: 53-57.

Oliveira, N.T.C. and A.C. Guastaldi, 2009. Electrochemical stability and corrosion resistance of Ti-Mo alloys for biomedical applications. Acta Biomater., 5: 399-405.

Peng, Q., B. Yang, L. Liu, C. Song and B. Friedrich, 2016. Porous TiAl alloys fabricated by sintering of TiH2 and Al powder mixtures. J. Alloys Compd., 656: 530-538.

Tamilselvi, S. and N. Rajendran, 2006. Electrochemical studies on the stability and corrosion resistance of Ti-5Al-2Nb-1Ta alloy for biomedical applications. Trends Biomater. Artif. Organs, 20: 49-52.